Chemosphere 364 (2024) 143143

Contents lists available at ScienceDirect

Chemosphere

journal homepage: www.elsevier.com/locate/chemosphere

Analysis of the effect of citrate on radionuclide retention on portlandite

Oscar Almendros-Ginesta [a,*], M Angeles Clavero-Sanchez [b], Miguel Sánchez [b], Tiziana Missana [a]

[a] CIEMAT Physical Chemistry of Actinides and Fission Products Unit, Spain
[b] Mass Spectroscopy and Geochemical Applications Unit, Avenida Complutense 40, 28040, MADRID, Spain

HIGHLIGHTS

- First study of radionuclide adsorption in portlandite in the presence of citrate.
- Citrate ($5{\cdot}10^{-3}$ M) decreases 40–50 times Pu and Eu uptake by portlandite.
- The effect of citrate on Ni and U adsorption is more limited (2–10 times).
- Thermodynamic databases predict minimal citrate/radionuclide complexation at pH = 12.5
- Citrate adsorption on portlandite is a mechanism inhibiting radionuclide retention.

GRAPHICAL ABSTRACT

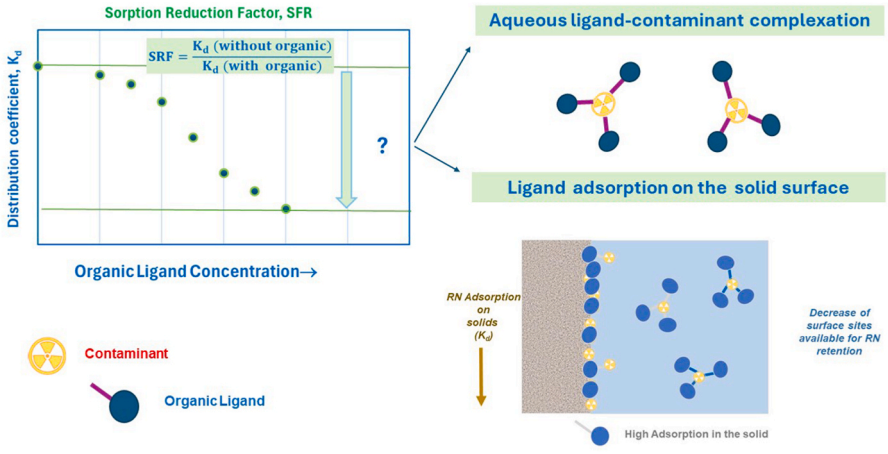

ARTICLE INFO

Handling editor: Milena Horvat

Keywords:
Cements
Radioactive waste
Adsorption
Organic ligands

ABSTRACT

We analysed how citrate (CIT), a chelating agent potentially present in radioactive waste disposals, affects the mobility of four radionuclides (RN): ^{63}Ni, ^{233}U, ^{152}Eu, ^{238}Pu in portlandite, an important hydrated phase of cement, a commonly used material for waste isolation.

Portlandite was synthetized in the laboratory and showed high purity and grain size of few μm. This solid, buffers the pH to 12.5 and shows high adsorption capability for the studied RNs: ^{152}Eu and ^{238}Pu exhibited the highest adsorption (K_d ~$1{\cdot}10^5$ mL g^{-1}) and ^{233}U the lowest (K_d ~$8{\cdot}10^2$ mL g^{-1}). CIT adsorption was also experimentally evaluated by batch sorption experiments and electrophoretic (ζ-potential) measurements: a non-lineal sorption behaviour was observed, with K_d values decreasing (from ~$1{\cdot}10^3$ mL g^{-1}) as CIT concentration increased up to $1{\cdot}10^{-2}$ M, according to portlandite sorption sites saturation.

In the presence of CIT, a marginal decrease for ^{233}U adsorption in portlandite was observed, one order of magnitude reduction for ^{63}Ni, while ^{238}Pu and ^{152}Eu adsorption decreased significantly. The calculated sorption reduction factors (SRF) for the four RN in the presence of CIT at a concentration of $5{\cdot}10^{-3}$ M were: 2.4, 9.7, 37 and 50.9 for ^{233}U, ^{63}Ni, ^{238}Pu, and ^{152}Eu, respectively.

According to the available thermodynamic databases, low complexation between CIT and RN is predicted at pH = 12.5, thus the RN adsorption decrease in the presence of CIT must be attributed to the organic adsorption

* Corresponding author.
E-mail address: oscar.almendros@ciemat.es (O. Almendros-Ginesta).

https://doi.org/10.1016/j.chemosphere.2024.143143
Received 29 April 2024; Received in revised form 30 July 2024; Accepted 19 August 2024
Available online 22 August 2024

on portlandite. However, current thermodynamic are still incomplete for this ligand and this pH range and this limits a precise interpretation of the experimental data.

1. Introduction

The disposal of radioactive waste is a complex topic, requiring robust solutions to protect both people and environment. Cement-based materials are widely used for confining and conditioning radioactive residues within disposal facilities. These materials present strong cohesive strength, and resilience over long time (Ochs et al., 2022); additionally they have low porosity and generate high pH, thus minimising radionuclide diffusion and favouring retention and precipitation processes (Grambow et al., 2020).

The interactions between cement and RN must be studied to assess the safety of radioactive waste disposals. These interactions are determined by the complex mineralogy of the cement, which is also impacted by the degradation of cementitious materials over the ages, produced by water filtration. The presence of additive of other co-stored residues may also play a role on RN mobility in the system. Adsorption is the process where a solute interacts with surface of solid, and can notably influence the mobility of contaminants, lowering the danger of environmental pollution. Therefore, RN adsorption studies are very important to assess the safety of the barrier materials in radioactive waste repositories.

Cementitious materials are formed by different hydrated phases (Ochs et al., 2022): calcium silicate hydrates (CSH), are the most common mineral phase in cement (60–70 wt%) (Duque-Redondo et al., 2021) being portlandite, $Ca(OH)_2$, the second most abundant presenting a 15 to 25 wt% of cement's structure.

The most common cement used worldwide, the ordinary Portland cement, OPC, initially establishes highly alkaline conditions (pH > 13), (Courland and Smith, 2011). As water comes in contact with the cement, the characteristics of the solid and its porewater change (Taylor, 1997). This degradation process is usually expressed using the variable of pH to define each degradation stage: the first stage (Stage I) is represented by the fresh cement, which buffers the pH up to 13.5, due to the presence of high quantity of alkaline elements, mainly sodium and potassium hydroxide phases. As far as these alkalis are diluted, pH decreases and the cement enters in the second stage of degradation (Stage II), where the pH is buffered to pH 12.5 by the mineral portlandite (Atkins and Glasser, 1992; Atkinson et al., 1989; Borkel, 2016; Galmarini and Bowen, 2016; Lee et al., 2021; Seewald and Seyfried, 1991). This buffering of pH follows the reaction E.1, controlling the Ca in cement pore water:

$$Ca(OH)_{2\ (s)} \rightleftharpoons CaOH^{+}_{(aq)} + OH^{-}_{(aq)} \rightleftharpoons Ca^{2+} + 2OH^{-}_{(aq)} \quad \text{E.1}$$

In Stage II, while portlandite is present in the system, the CSH remain stable. When portlandite is entirely consumed, the systems enters in the third stage of degradation, where CSH dissolves progressively, buffering the pH down to 10.5 (Atkins and Glasser, 1992; Atkinson et al., 1989; Seewald and Seyfried, 1991). Once CSH are finally dissolved, further buffering of the pH depends on the cement system remaining (Borkel, 2016).

The objective of this study is to analyse the adsorption of four different radionuclides ^{233}U(VI), ^{238}Pu(IV), ^{152}Eu(III) and ^{63}Ni(II) on portlandite, which is the most important mineral in the Stage (II) of cement degradation and to evaluate the potential effect of the presence of citrate on their retention.

Nickel, can be found in low- or intermediate-level radioactive waste (LILRW) following the decommissioning of metallic materials present in the structural components of nuclear reactor vessel (Carboneau and Adams, 1995). On the other hand, uranium's main use is nuclear fuel production, hence its presence in radioactive waste material must be considered. Europium and plutonium are representative (or homologue) of tetra- and tri-valent actinides. Plutonium presence in radioactive waste is product of fission from nuclear fuel. Europium can be produced because neutron activation of control rods in nuclear reactors and as a fission product of U and Pu (Ochs et al., 2022). Furthermore, due to their different valence, they represent good example of the behaviour of various chemical species present in the wastes.

Citric acid (CIT) can be found in these wastes because its presence in decontamination sludge. This is because the use of CIT for radioactive decontamination in nuclear plants decommissioning as a RNs chelating agent (IAEA, 2001), allowing for RN recovery and waste minimization from the contaminated site. Furthermore, due to its capacity of chelating Ca ions, citric acid could be also used in cement as retarder (Belhadi et al., 2021; Kastiukas et al., 2015; Zhang et al., 2016; Zou et al., 2020) altering the kinetics of hydration reactions, slowing down the setting and hardening of the cement mixture.

The interactions of CIT with radionuclides or heavy metals have been largely studied in the past, for the possible use of this organic in soils decontamination (Duarte et al., 2007; Gavrilescu et al., 2009; Turgut et al., 2004) or to understand its possible role on hazardous ion migration in the environment (Bonin et al., 2008; Lenhart et al., 2000).

Previous studies showed that CIT is an important complexing agent (Hummel et al., 2005) and that could play an important role towards ^{233}U and ^{63}Ni migration (Byrd et al., 2021). This interaction between RN - CIT may cause a coordination of an adsorbing metal by an organic ligand in the solution, competing with the metal binding (sorption) on solid phases (Loon and Glaus, 1998).

Radionuclide sorption studies in the presence of citric acid on different materials as alumina (Pasilis and Pemberton, 2008), silica (Kar et al., 2012), iron oxides (Engel et al., 2021) or clays (Verma et al., 2015), have been reported. However, most of these studies were performed under acidic or slightly alkaline conditions, and to the best of our knowledge, no previous works analysed the effect of citric acid on radionuclide adsorption on portlandite, under the hyper alkaline conditions generated by cements.

In this study, the binary RN-portlandite and CIT-portlandite systems were evaluated first, analysing separately the adsorption of the RN and the organic on the portlandite by adsorption isotherms under the widest as possible range, as to evidence adsorption and precipitation processes. Secondly, the effect of increasing CIT concentration on the adsorption of the selected RN in portlandite has been experimentally determined, to calculate the reduction sorption factors i.e: the ratios between the distribution coefficients, K_d, of the RN in the solid in the presence/absence of the ligand.

Geochemical modelling has been used to interpret the experimental results trying to evaluate the impact of the aqueous complexation of the organic with the RN and the role of CIT adsorption on portlandite. The limitation of modelling caused by the shortage of thermodynamic data has been discussed.

2. Materials and methods

2.1. Portlandite synthesis and characterisation

Portlandite ($Ca(OH)_2$(s)) has been obtained by recrystallization of dissolved CaO(s) in purged water and ultrapure water, following the equation:

$$CaO(s) + H_2O \rightleftharpoons Ca(OH)_2(s) \quad \text{E.2}$$

The synthesis and drying of the solid carried out inside glove box under N_2 atmosphere to prevent the carbonation of the solid.

Once dried, the solid was crushed and suspended in 20 mM Ca $(OH)_2$(aq), with a pH of 12.5 ± 0.1, being this is the equilibrium solution with the portlandite. The solid to liquid ratio used in the experimental

work was 1 g L^{-1}. Portlandite particle size in solution was determined by dynamic light scattering (DLS) using the NanoBrook 90Plus Zeta (Brookhaven Instrument Corporation) particle size analyzer.

The solid was analysed by attenuated total reflection Fourier transform infrared spectroscopy (ATR-FTIR) with a Nicolet iS50 equipment and X-ray diffraction, XRD, with an Axios spectrometer from Panalytica, confirming that the synthesis proceeded adequately. For the microstructural characterization of the solid, scanning electronic microscope (SEM) was used with an electron microscope JSM6400 (JEOL).

2.2. Organic ligand

The citric acid (CAS: 77-92-9, C_6H_8O7, MW: 192.12 g mol^{-1}, ACS ≥99.5) was purchased as powdered reagent (Sigma Aldrich) and the initial solutions for the experimental work were prepared with deionized water (DW) with concentrations from 0.001 to 1 mol L^{-1}. Citrate in solution was determined by ion chromatography. Two ion chromatographs Dionex ICS-2000 RFIC and Dionex AQUAION RFIC were used. The anions analytical columns included a guard column Dionex AG19 and a separator column Dionex AS19 (THERMO SCIENTIFIC).

2.3. Radionuclides

The radionuclides (RN) used for the experiments were ^{63}Ni(II), ^{233}U (VI), ^{152}Eu(III) and ^{238}Pu(IV). Details of the initial solutions, used in the experiments, are described in Table 1. To reach a wider range of concentrations for the Ni, U and Eu isotherms, stable chemical of high purity were added to the radioactive isotope ($NiCl_2$, $UO_2(NO_3)_2{\cdot}6H_2O$, $Eu(NO_3)_3{\cdot}5H_2O$).

2.4. Batch sorption experiments

Batch sorption tests in portlandite (1 g L^{-1}) where carried out in the electrolyte in equilibrium with this solid phase: 20 mM $Ca(OH)_2$(aq)). The experiments were done inside glove-box under N_2 atmosphere at a temperature of 22 ± 2 °C. The selected contact time for the adsorption tests with and without the presence of organic was 7 days. Kinetic effects possibly caused by long-term structural changes of portlandite, were not considered here.

Sorption isotherms were carried out with the RNs, within the concentration range indicated in Table 1.

The main objective of the sorption isotherms was to determine the operational solubility of each radionuclide under the selected experimental conditions, evidencing the concentration ranges in which adsorption or precipitation occurs.

After the selected contact time, the solid and liquid phases were separated by centrifuging (21255 g, 30 min), with a JOUAN MR23i centrifuge. Three aliquots of the separated liquid were extracted from each tube for the analysis of the final RN activity. The activity of alpha-beta emitters was measured with a liquid scintillation analyser Tri-Carb 4910 TR (PerkinElmer) and using Ultima Gold™ as a scintillation cocktail. The activity of gamma emitters was measured with Autogamma Cobra II 5003 (Packard) with 3″ detector of NaI (TP). The uncertainty for the counting procedure is less than 2%. Under the experimental conditions the adsorption of all the radionuclides in the centrifuge tubes is negligible.

Table 1
Details of the initial conditions of batch sorption tests on portlandite. pH = 12.5 ± 0.1; Ca = 20 mM. Solid to liquid ratio 1 g L^{-1}.

Radioisotope	Solutions	[RN] for sorption isotherms (M)	[RN] for tests with CIT (M)	Log(K_d) without CIT (±0.2)[a]
^{63}Ni	$NiCl_2$ in 0.1 M HCl	[$4{\cdot}10^{-10}$ – $5{\cdot}10^{-7}$]	$1.1{\cdot}10^{-9}$	3.5
^{233}U	$UO_2(NO_3)_2$ in 4 M HNO_3	[10^{-7} - 10^{-3}]	$2.4{\cdot}10^{-7}$	3.0
^{152}Eu	$EuCl_3$ in 0.1 M HCl	[$7{\cdot}10^{-10}$ – 10^{-7}]	$2.0{\cdot}10^{-10}$	5.5
^{238}Pu	$Pu(NO_3)_4$ in 4 M HNO_3	[$7{\cdot}10^{-11}$ - $9{\cdot}10^{-9}$]	$1.7{\cdot}10^{-10}$	5.1

[a] ±0.2 is the maximum error on Log(K_d) observed in all sorption tests.

Sorption isotherms were also carried out with CIT on portlandite, using a CIT concentration from 10^{-5} to 10^{-2} M. In these experiments, the solid and liquid phases were separated within the glove box using 0.2 μm filters from Millex-GN™.

The analysis of the effect of CIT on RN retention was carried out fixing the RN concentration ([^{63}Ni] = $1.1{\cdot}10^{-9}$ M, [^{233}U] = $2.4{\cdot}10^{-7}$ M, [^{152}Eu] = $2.0{\cdot}10^{-10}$ M and [^{238}Pu] = $1.7{\cdot}10^{-10}$ M, Table 1), according to the previous sorption isotherms to ensure that adsorption (and not precipitation) is the main RN retention mechanism, and increasing the concentration of CIT from 10^{-5} to 10^{-2} M.

The distribution coefficient (K_d), used to quantify the extent of RNs or CIT adsorption on portlandite, is defined as:

$$K_d = \frac{[C]solid}{[C]eq} \cdot \frac{V}{m} \quad \text{E.3}$$

In the usual K_d definition, $[C]_{eq}$ represents the concentration of the adsorbate remained in the aqueous phase at the equilibrium, $[C]_{solid}$ is the adsorbate concentration retained in the solid ($[C]_{in}$ - $[C]_{eq}$), V the volume of the solution [mL] and m the mass of the solid [g]. The error is calculated as the standard deviation of the measurements for the repetitions (at least three) of the same sample.

For a practical point of view, it is of interest to determine the sorption reduction factor, SRF, in the presence of organics, which indicates the capability of the organic (ORG) of decreasing the RN uptake, and is given by the ratio (Burešová et al., 2023; Ochs et al., 2022):

$$SRF = \frac{Kd(RN\ without\ ORG)}{Kd\ (RN\ with\ ORG)} \quad \text{E.4}$$

The concentration of CIT considered for calculating the SRF value is $5{\cdot}10^{-3}$ M.

2.5. ζ-potential measurement

The analysis of the variation of the electro kinetic potential (ζ-potential) under different chemical conditions is of great support in adsorption studies. As the solubility of the RN under the chemical conditions generated by portlandite is very low, these electrophoretic measurements were carried out only for supporting CIT adsorption studies.

The ζ-potential of the portlandite (1 g L^{-1} in 20 mM $Ca(OH)_2$ (aq)) in the presence of CIT ($5{\cdot}10^{-6}$ to 10^{-2} M) was measured by Laser Doppler electrophoresis, with a Malvern Zetamaster apparatus equipped with a He–Ne laser (λ = 633 nm). The preparation of the samples was carried out in the anoxic glove box and the samples were taken out from the chamber into a syringe just before measurement. The measurements were done upon approximately 1 h and after 30 days of CIT and portlandite contact time.

2.6. Modelling

Modelling calculations were done using the geochemical software CHESS (Chemical Equilibrium of Species and Surfaces) (Van der Lee and de Windt, 1999). The software is used in many specific areas, mainly in environmental engineering, performance and safety assessment of waste repositories, grout, and surface water pollution studies.

The thermodynamic database used for calculating RN and CIT speciation and modelling CIT and RN sorption on portlandite, is the Andra (French National Radioactive Waste Management Agency), NWS

(Nuclear Waste Services, UK) and ONDRAF-NIRAS (Belgian Agency for Radioactive Waste and Enriched Fissile Materials, Belgium) Thermochimie database (TC DB) v12a (Giffaut et al., 2014). This is one of the most complete and up to date database available nowadays (Giffaut et al., 2014), for RN, which is mainly based on the Nuclear Energy Agency's database (NEA DB). Speciation plots obtained for the studied conditions and each species are shown in the Supplementary Material.

The RN and/or CIT sorption modelling on portlandite is based on the surface complexation model proposed by (Almendros-Ginestà et al., 2023) (E.5, E.6; Table 2) based on a simplified double layer approximation to describe the portlandite surface site chemistry, assuming that Ca is the ion determining the potential. Using this approximation, the solid surface interaction with RN can be described, allowing the possibility to propose surface complexes that may describe the experimental adsorption data.

$$S\text{–}OH \rightarrow S\text{–}O^- + H^+ \quad \text{E.5}$$

$$S\text{–}O^- + Ca^{2+} \rightarrow S\text{–}O\text{–}Ca^+ \quad \text{E.6}$$

3. Results and discussion

3.1. Portlandite characterization

Attenuated total reflection Fourier transform infrared spectroscopy and X-ray diffraction, shown in the Supplementary Material (Fig. S1), demonstrated that the synthetized solid is pure portlandite. The size of portlandite particle in solution (20 mM Ca(OH)2), measured by DLS, indicated the existence of aggregate with size larger than 3 μm, out from the colloidal size range. SEM analysis also indicated a well crystallized material with a grain size of few micrometres, as clearly shown in Fig. 1.

3.2. RN adsorption isotherms on portlandite

Fig. 2 shows the adsorption isotherms of ^{63}Ni, ^{233}U, ^{152}Eu and ^{238}Pu expressed as the logarithm of the adsorbed concentration Log(C_{ads}) ([C_{ads}] in mol·g^{-1}) *vs.* the logarithm of the equilibrium concentration in solution, Log(C_{eq}) ([C]$_{eq}$ in mol·L^{-1}.

In these isotherms, the lines with slope 1, drawn in the Figure, indicates the region of linear adsorption, where the distribution coefficient, K_d, remains constant. When the slope of the isotherm is higher than 1, precipitation occurs, which also revealed by a sudden increase of the K_d values.

Table 2
Reactions used for simulating adsorption processes in portlandite. The LogK is referred to the description of the surface complex in the CHESS code. Data and reactions with (*) has been already presented in (Almendros-Ginestà et al., 2023).

Reaction		Species description (CHESS Code)	LogK
E.5	$S\text{–}OH \rightarrow S\text{–}O^- + H^+$	1 S–OH, −1 H^+	−6.8 ± 0.20*
E.6	$S\text{–}O^- + Ca^{2+} \rightarrow S\text{–}O\text{–}Ca^+$	1 S–OH, −1 H^+, 1 Ca^{2+}	−3.6 ± 0.20*
E.7	$S\text{–}O^- + Eu(OH)_2^+ \rightarrow S\text{–}O\text{-}Eu(OH)_2$	1 S–OH, −3 H^+, 1 Eu^{3+}, 2 H_2O	−12.95 ± 0.20*
E.8	$S\text{–}O^- + Pu(OH)_3^+ \rightarrow S\text{–}O\text{-}Pu(OH)_3$	1 S–OH, −4 H^+, 1 Pu^{4+}, 3 H_2O	+4.35 ± 0.20*
E.9	$S\text{–}O\text{–}Ca^+ + Ni(OH)_3^- \rightarrow S\text{–}O\text{–}Ca\text{–}Ni(OH)_3$	1 S–OH, −4 H^+, 1 Ca^{2+}, 1 Ni^{2+}, 3 H_2O	−31.25 ± 0.20
E.10	$S\text{–}O\text{–}Ca^+ + UO_2(OH)_4^{2-} \rightarrow S\text{-}O\text{-}Ca\text{-}UO_2(OH)_4^-$	1 S–OH, −5 H^+, 1 Ca^{2+}, 1 UO_2^{2+}, 3 H_2O	−32.04 ± 0.20
E.11	$S\text{–}O\text{–}Ca^+ + Cit^{3-} \rightarrow S\text{–}O\text{–}Ca\text{-}Cit^{2-}$	1 S–OH, −1 H^+, 1 Ca^{2+}, 1 Cit^{3-}	+2.25 ± 0.20

*BET = 13.4 m^2/g.
*Site density = 3.84 μmol/m.^{2}.

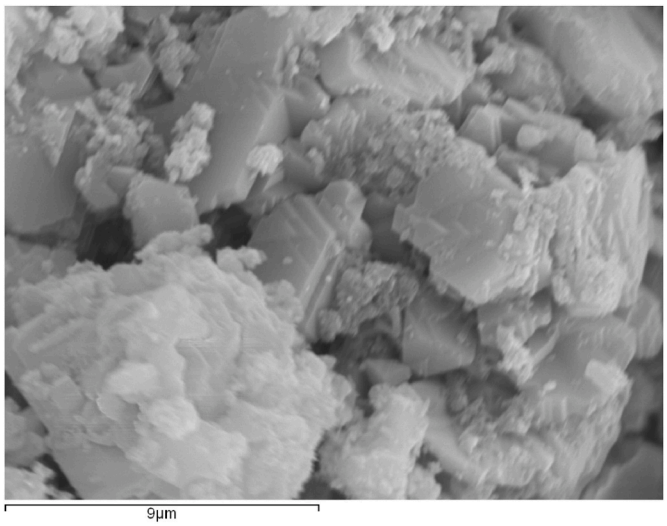

Fig. 1. SEM Picture of synthetized portlandite.

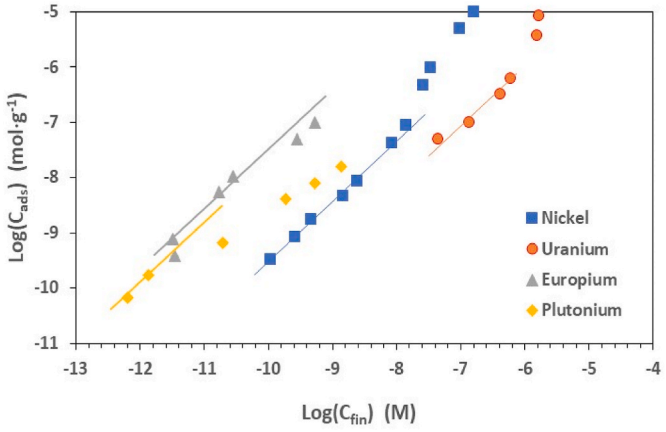

Fig. 2. Adsorption isotherms of (■) ^{63}Ni (●); ^{233}U (▲); ^{152}Eu (◆); ^{238}Pu on portlandite (1 g L^{-1}) in 20 mM Ca(OH)$_2$(aq). Details on experimental conditions are shown in Table 1.

For ^{63}Ni, sorption is linear until an equilibrium concentration of approximately 2.5·10^{-8} M (initial concentration of 5·10^{-7} M), then precipitation occurs; in the linear region, the Log(K_d) is around 3.5 (K_d ~3200 mL g^{-1}). In the case of ^{233}U, adsorption is linear up to an equilibrium concentration of 1.6·10^{-6} M and the Log(K_d) is approximately 2.9 (K_d ~800 mL g^{-1}); at higher concentration also uranium precipitation occurs. Within the range of concentration analysed, ^{152}Eu shows linear sorption with a Log(K_d) of approximately 5.5 (K_d ~3.7·10^5 mL g^{-1}). In the case of ^{238}Pu, the zone of linear sorption is limited to very low concentrations (<10^{-12} M) with a Log(K_d) of approximately 5 (K_d ~1.3·10^5 mL g^{-1}).

The theoretical solubility of the different elements under the experimental conditions (20 mM Ca(OH)$_2$ and pH = 12.5) was analysed with the Chess code. The solid determining the solubility were: Ni(OH)$_2$(s) (2.8·10^{-8} M); Bequerelite (Ca(UO$_2$)$_6$O$_4$(OH)$_6$:8H$_2$O, (8.2·10^{-7} M); Eu(OH)$_3$(am) (3.0·10^{-9} M) y PuO$_2$ (s) (1·10^{-12} M), for Ni(II), U(VI), Eu(III) and Pu(IV), respectively. Assuming these solids, the onset of precipitation, observed in the sorption isotherms, agrees very well with the theoretical values for Ni, U and Eu solubility. In principle, Pu(IV) should precipitate at concentrations higher 10^{-12} M, but in the adsorption isotherms we do not observe clear signs of precipitation, as we did in the case of Ni or U. Nevertheless, the decrease in slope in the isotherm for higher Pu concentrations can be related to the presence of Pu colloids,

that were not well separated by centrifuging (Almendros-Ginestà et al., 2023).

The values of Log(K_d) obtained for each RN in this region are summarized in Table 1, and represent the reference values of adsorption without the presence of CIT. Adsorption is the highest for ^{152}Eu and ^{238}Pu and the lowest for ^{233}U.

3.3. CIT sorption isotherm on portlandite

Fig. 3 shows the adsorption isotherms of CIT, expressed as the logarithm of the distribution coefficient (K_d) *vs.* the logarithm of the equilibrium concentration of CIT (Log[CIT]) in the solution at the equilibrium.

The range of CIT concentration was relatively short, starting from $5{\cdot}10^{-5}$ M, due to the detection limit of the technique used. Within this concentration range, a progressive decreasing of the Log(K_d) is observed, possibly due to the saturation of portlandite sorption sites. The maximum measured Log(K_d) is approximately 2.96 (K_d~912) which rapidly decreases up to approximately 1.64 (K_d~44) before the sharp increase, at concentrations higher than $1{\cdot}10^{-3}$ M, attributable to CIT precipitation, being the solubility of the calcium citrate $[Ca_3(C_6H_5O_7)_2]\cdot 2H_2O$ approximately 1 g L^{-1} at 25 °C.

Within the range investigated, the adsorption of CIT on portlandite is not negligible, even if the K_d values are lower than those observed for all the radionuclides (Table 1), and especially when the organic concentration is higher. Furthermore, the CIT precipitation observed is expected to limit the formation of aqueous RN-CIT complexes if the CIT concentration exceed approximately $1{\cdot}10^{-3}$ M.

Comparing the results from Fig. 3 with other literature data (Guidone et al., 2024), CIT sorption presents higher K_d values than other cement mineral phases like ettringite or CSH. The high positive charge of the portlandite in respect to the other mineral phases, and the presence of Ca^{2+} which can bridge the surface interactions, are most probably the responsible of this high CIT adsorption in portlandite.

Fig. 4 shows the variation of portlandite ζ-potential in the presence of increasing concentration of CIT, data which provide very useful information for the interpretation of CIT-portlandite interactions. Fig. 4a shows the results at low CIT concentration ($5{\cdot}10^{-6}$ M to 10^{-3} M), with the concentration expressed in a logarithmic scale to make more evident the changes, and in Fig. 4b the results in the entire range of concentration are shown, to depict the overall behavior. In the Figure, open points represent measurements performed upon 1 h of contact between CIT and portlandite and closed point the measurements performed on the same samples upon 30 days.

The results obtained at two different contact times are very similar, indicating that the adsorption of CIT in the portlandite is very rapid and

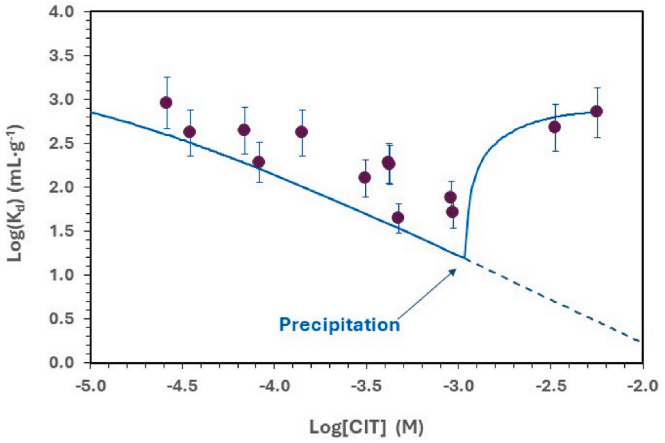

Fig. 3. CIT adsorption isotherm on portlandite (1 g L^{-1}) in 20 mM Ca$(OH)_2$(aq). The continuous line corresponds to the modelling of CIT adsorption.

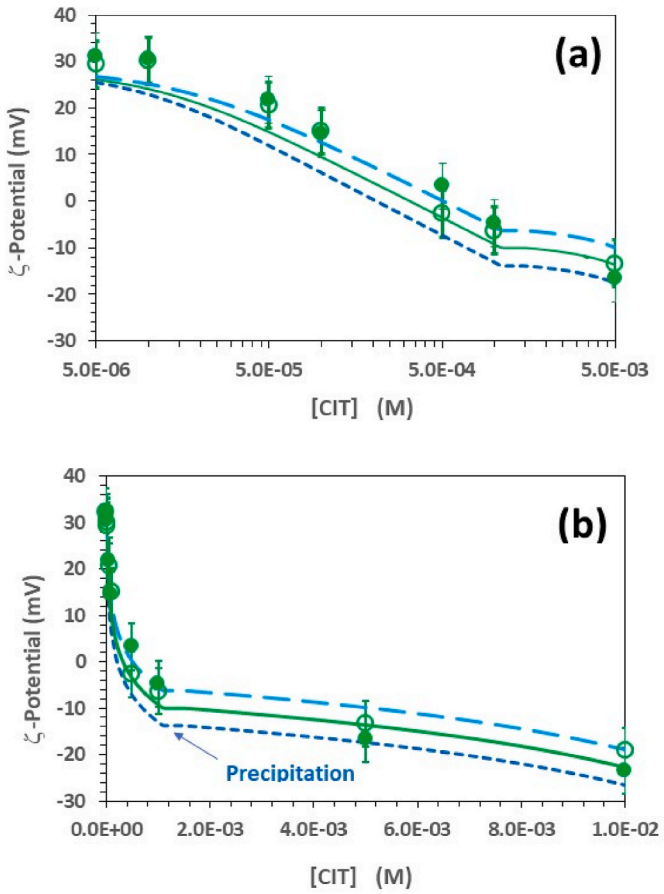

Fig. 4. ζ-potential of portlandite (1 g L^{-1}) in 20 mM Ca$(OH)_2$(aq)as a function of the CIT concentration. Open points correspond to the measurements carried out upon 1 h of contact and closed points to the measurements upon 30 days. The different lines correspond to a sensitivity study on the LogK of the formation of the complex of the CIT with the portlandite surface (E.11). The continuous green line corresponds to LogK = 2.25; the dashed cyan line corresponds to the value of LogK = 2.05; the dotted blue line correspond to the value of LogK = 2.45. (For interpretation of the references to colour in this figure legend, the reader is referred to the Web version of this article.)

that the interaction is not affected by kinetics.

As reported in (Almendros-Ginestà et al., 2023), the initial ζ-potential of the portlandite in 20 mM Ca$(OH)_2$(aq) is positive (~30 mV) at pH 12.5. The positive ζ-potential is expected to favor surface interaction with negatively charged species, like CIT, so this may explain the relatively high adsorption of the organic observed in Fig. 3.

The increase of the CIT concentration causes a significant decrease of the ζ-potential that turns negative for CIT concentrations higher than $5{\cdot}10^{-4}$ M (Fig. 4a). The rapid decrease of the portlandite surface potential in the presence of CIT can be indeed attributed to CIT adsorption, and possibly indicates the formation of a negatively charged surface complex. However, as observed in Fig. 3, the data obtained at CIT concentrations higher than $1{\cdot}10^{-3}$ M must be affected by CIT precipitation in solution.

3.4. Adsorption of RN on portlandite with the presence of CIT

Fig. 5 shows the adsorption of the for RNs in the presence of increasing concentrations of CIT at fixed RN concentrations (Table 1) to evaluate the effect of CIT in the RN linear sorption zone. Considering the previous results, to avoid undesirable effects of CIT precipitation, the RN sorption tests were done increasing the CIT concentration only up to $5{\cdot}10^{-3}$ M. Additionally, very high concentrations of CIT may produce

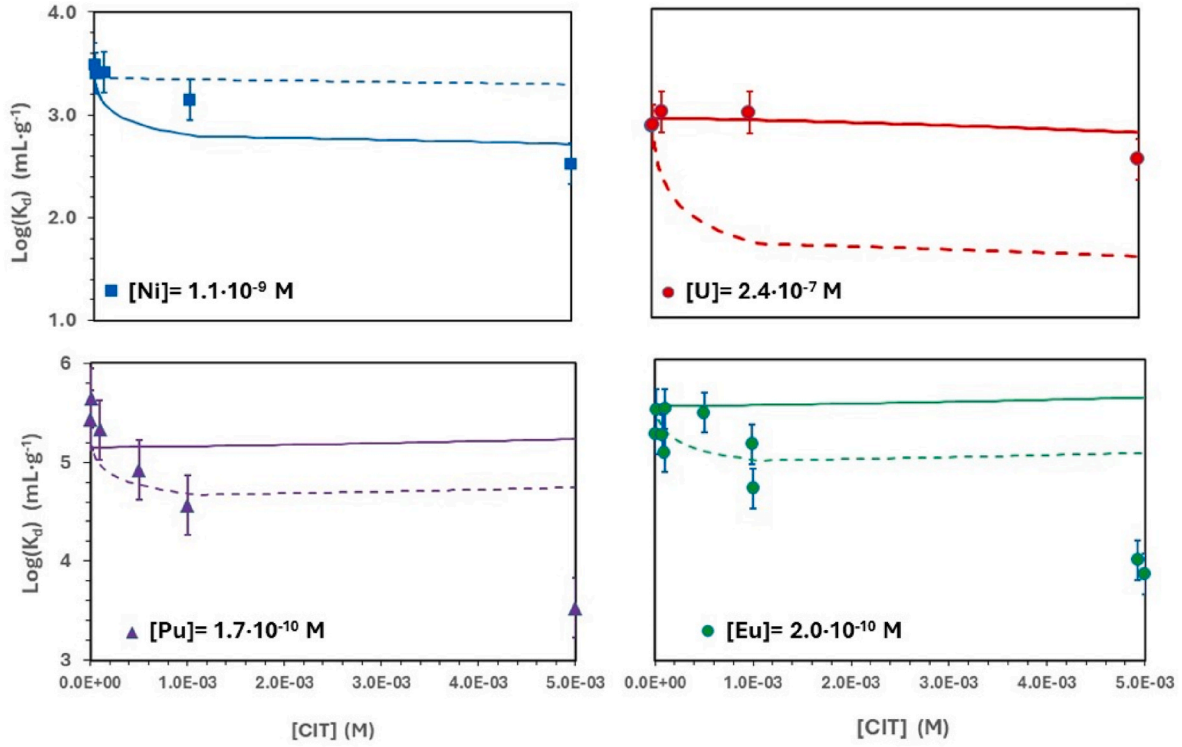

Fig. 5. RN adsorption in portlandite (1 g L^{-1}) in the presence of CIT. Continuous lines correspond to the calculation which considers only the effect of the formation of aqueous RN-CIT complexes, the dotted line shows the calculations including the CIT adsorption on portlandite.

dissolution of the solid also biasing the adsorption results. At concentrations above $5{\cdot}10^{-3}$ the solid dissolves about 20% from the initial solid-liquid concentration. This did not affect the final calculations.

These results in Fig. 5, indicate moderate to negligible effect of CIT on ^{233}U and ^{63}Ni adsorption on portlandite, while stronger effect is seen for ^{152}Eu and ^{238}Pu. Data reported in Fig. 5 have been also plotted with the CIT concentration expressed in logarithmic form, to better evidence the effect of citrate at low concentrations, and the Figure is provided in the supplementary material (Fig. S2).

In the presence of $5{\cdot}10^{-3}$ M, the K_d for ^{63}Ni decreases approximately one order of magnitude (K_d from approximately 3200 mL g^{-1} to 330 mL g^{-1}), whereas for ^{233}U the decrease is more limited (K_d from approximately 800 mL g^{-1} to 340 mL g^{-1}). For ^{152}Eu, K_d values decrease from $3.67{\cdot}10^5$ mL g^{-1} to 7200 mL g^{-1}, and, in the case of ^{238}Pu, from $1.3{\cdot}10^5$ mL g^{-1} to 3400 mL g^{-1}.

The SRF, were calculated to quantitatively indicate the effect of CIT in sorption tests, considering the highest concentration of CIT used in these tests ($5{\cdot}10^{-3}$ M). The results are summarized in Table 3.

The decrease in sorption in the presence of organics might be attributed to the formation of RN-CIT aqueous complexes, which remain stable in solution preventing RN interaction with the solid, but also to the adsorption of the organic blocking surface sites and acting in competitive way. The role of these possible processes will be theoretically analysed with the aid of geochemical modelling.

Table 3
SRF values calculated for the different RN in the presence of [CIT] = $5{\cdot}10^{-3}$ M.

RN	RN concentration	K_d (without CIT) (mL·g^{-1})	K_d (with CIT) (mL·g^{-1})	SRF
^{63}Ni	$1.1{\cdot}10^{-9}$	**3200**	**330**	**9.7**
^{233}U	$2.4{\cdot}10^{-7}$	**800**	**340**	**2.4**
^{152}Eu	$2.0{\cdot}10^{-10}$	**367000**	**7200**	**50.9**
^{238}Pu	$1.7{\cdot}10^{-10}$	**128300**	**3400**	**37.7**

4. Modelling

Geochemical calculations of the RN-portlandite-CIT system were carried out with the databases available for the analysed RN and CIT complexes in the NEA DB (Hummel et al., 2005) and the TC DB. For calculating the speciation of Ni, the values recently provided by (Gonzalez-Siso et al., 2018) have been also included.

It must be noted that data for the Eu-CIT and Pu-CIT complexes are not available, therefore calculations were carried out with the data of analogues elements (Am-CIT and Th-CIT).

First, the calculation of the speciation of CIT and the radionuclides under the chemical conditions generated by portlandite (pH = 12.5 and 20 mM Ca^{2+}) were carried out. In the case of the RN, the speciation without and with CIT was also compared; all the results from these calculations are provided in the Supplementary Material.

Fig. S3 in the Supplementary Material shows the speciation of CIT in 20 mM $Ca(OH)_2$(aq), where it can be observed that the main calculated species at pH = 12.5 is Ca(Cit)[−] (98.8 %) and Cit[3-] (1.2 %) is also present, both negatively charged.

Fig. S4 shows the ^{63}Ni speciation in 20 mM $Ca(OH)_2$ (aq), without (Fig. S2a to Fig. S4a) and with (Fig. S2b to Fig. S4b) CIT ($1{\cdot}10^{-2}$ M). At pH 12.5, the main ^{63}Ni species are the $Ni(OH)_2$ (aq), (90.2 %) and the negatively charged $Ni(OH)_3$[-] (9.8%), which could interact with the positively charged portlandite surface. The main CIT-Ni species (Fig. S2b) is Ni(Cit)[−], that according to the database, is present only in a minor concentration at pH 12.5.

Fig. S5 shows the ^{233}U speciation in 20 mM $Ca(OH)_2$(aq) without (Fig. S23 to Fig. S5a) and with (Fig. S3b to Fig. S5b) the presence of CIT ($1{\cdot}10^{-2}$ M). At pH 12.5, the main ^{233}U species are the negatively charged $UO_2(OH)_4$ [2-] (79.81 %) and $UO_2(OH)_3$[-] (20.19%). In the presence of CIT, no U-CIT species are present in the range of pH from 10 to 13 and the speciation is very similar to that observed without citric acid.

Fig. S6 shows ^{152}Eu speciation in 20 mM $Ca(OH)_2$(aq) without and with CIT presence of $5{\cdot}10^{-3}$ M, because the speciation is the same for both systems. The main ^{152}Eu species at pH 12.5 is $Eu(OH)_3$ (97.60%)

and $Eu(OH)_2^+$ (1.2%) as the charged specie. In the presence of CIT, no Eu-CIT specie is formed in the working conditions nor in the pH range from 10 to 13.

Fig. S7 shows ^{238}Pu speciation in 20 mM $Ca(OH)_2$(aq) without and with CIT presence of $5{\cdot}10^{-3}$ M, because, yet again, the speciation is the same for both systems. The main ^{238}Pu specie at pH 12.5 is $Pu(OH)_4$ (>99%) and $Pu(OH)_3^+$ (<1%) as the charged specie. In the presence of CIT, no Pu-CIT specie is predicted in the conditions of our study nor in the pH range from 10 to 13.

To simulate RN adsorption experiments without the CIT, the model described in (Almendros-Ginestà et al., 2023) was used, considering the formation of the surface complexes indicated in Table 2. The first two equations (E.5 and E.6) represent the deprotonation reaction of the generic surface site SOH, and its complexation with Ca (SOCa[+]), the ion determining the potential of the portlandite. The other equations represent the RN-surface complexes formation (for ^{152}Eu: Eq. (7); ^{238}Pu: Eq. (8); ^{63}Ni: Eq. (9)and for ^{233}U: Eq. (10)), considering the mayor charged species present in solution, according to speciation. The constant is determined by fit the calculated K_d with the experimental ones of the linear zone of the isotherm.

Fig. S6

Furthermore, these calculations reproduced very well the onset of precipitation, being the solids limiting the solubility $Ni(OH)_2$(s) or $CaU_2O_7{\cdot}3H_2O$(cr) for ^{63}Ni and ^{233}U respectively.

For simulating the adsorption of CIT in the portlandite both the adsorption and the ζ-potential data were considered. As observed in Fig. S1 to Fig. S3, the main CIT species predicted in the system is the Ca(Cit)$^-$. As Ca(Cit)$^-$ is the major species, we initially considered the formation of a surface complex with portlandite this species, namely:

$$S\text{–}O\text{–}Ca^+ + CaCit^- \rightarrow S\text{–}O\text{–}Ca\text{-}CaCit \qquad E.12$$

However, using this hypothesis, it was not possible to simulate well both electro kinetic and sorption data. Taking into account the rapid decrease of the ζ-potential of the surface charge of portlandite in the presence of CIT, we probably must assume the formation of a negatively charged surface complex, thus we considered the adsorption of the basis specie (Cit^{3-}), forming the following surface complex:

$$S\text{–}O\text{–}Ca^+ + Cit^{3-} \rightarrow S\text{–}O\text{-}CaCit^{2-} \qquad E.11$$

Considering the formation of this surface complex, and assuming a maximum possible variation of LogK, between 2.45 and 2.05 (mean 2.25 ± 0.2), both sorption and electrophoretic data could be simulated. The simulation of CIT sorption on portlandite data in Fig. 3 has been obtained using the value of LogK for E.11 of 2.1.

In Fig. 4a and b, the continuous lines correspond to the fit of the ζ-potential data assuming the adsorption reaction (E.11) with the mean value of LogK (2.25), whereas the light blue and blue dotted lines correspond with the minimum and maximum values of LogK possible (2.05 and 2.45) obtained in the sensitivity analysis performed.

To understand which can be the main causes of the decrease in adsorption produced by the presence of CIT (Fig. 5), on ^{63}Ni, ^{233}U, ^{152}Eu and ^{238}Pu adsorption on portlandite, the experimental data in Fig. 5, were analysed considering: a) the effect of the formation of aqueous RN-CIT complexes and b) the contribution of CIT uptake by the solid, by blocking of sorption sites. The performed calculations are superimposed to the experimental points in Fig. 5 a continuous line for (a) and with a dotted line for (b).

Due to the very small interactions between RN and CIT observed under the conditions generated by the portlandite, the possible contribution of ternary complexes was discarded, trying to not over interpret the experimental results.

As observed by in the RN speciation calculations in the presence of the organic ligand (Figs. S2–S5), the extent of the formation of RN-CIT complexes at pH = 12.5 and Ca = 20 mM is limited, therefore according to the database, a significant effect of the aqueous RN-CIT complexation is not expected. In fact, the calculations made using the hypothesis (a) do not predict any significant K_d change as a function of CIT concentration (continuous lines in Fig. 5), which agrees only with the experimental data of ^{233}U.

However, experiments shows that a reduction in the K_d values is observed in the presence of CIT (Table 3), especially for ^{152}Eu and ^{238}Pu which must be attributed to other mechanisms.

To check the potential contribution of CIT retention at the portlandite surface, the equation representing CIT adsorption (E.11, Table 2) was included in the calculations. In this case, a decrease of sorption is predicted (about one order of magnitude), which agrees with the experimental data for ^{63}Ni, but still underpredict the decrease in K_d at the highest concentration of CIT for ^{152}Eu and ^{238}Pu. In the case of ^{233}U, the addition of CIT sorption contribution worsens the initial simulation.

Thus, even if the adsorption of CIT may represent a contribution on the overall RN sorption in the presence of citrate the model is not completely satisfactory, and it is not able to reproduce the SRF values at the highest CIT concentration.

To perform more precise calculations and gain predictive capability an important effort must be devoted to the obtention of complete and accurate thermodynamic databases: for example, for Pu and Eu complexes but also for U, data which have been recently changed in the Thermochimie database (from v.10 to v.12) and not yet included in the NEA database.

5. Conclusions

In this study, we analysed the adsorption of ^{63}Ni, ^{233}U, ^{152}Eu, ^{238}Pu and CIT in portlandite and the effect of the presence of CIT on radionuclide adsorption. The effect of the ligand (at a concentration of $5{\cdot}10^{-3}$ M) is practically null for ^{233}U sorption and, while visible, is limited also for ^{63}Ni. Nevertheless, an important decrease for ^{152}Eu and ^{238}Pu K_d values (40–50 times) is observed.

According to the available thermodynamic databases the formation of CIT-RN complexes is negligible under the conditions generated by portlandite (pH = 12.5 and Ca = 20 mM), thus we must assume the existence of other mechanisms producing the decrease of RN sorption in the presence of CIT, when experimentally observed. Considering the competitive CIT adsorption on the portlandite surface, a decrease of K_d values is predicted, which agrees very well with the ^{63}Ni data; however, the predicted decrease is still low than the experimental for ^{152}Eu and ^{238}Pu.

To analyse the data and perform detailed calculations thermodynamic databases are needed. Pu(IV)-CIT complexes are non-existent in the current databases, hence species of Th(IV)-CIT were used. Likewise, Eu(III)-CIT were analogues of Am(III)-CIT species. The shortness of thermodynamic data for organic-radionuclides species under hyperalkaline conditions is a limiting factor for a more mechanistic description of the experimental results.

CRediT authorship contribution statement

Oscar Almendros-Ginesta: Writing – review & editing, Writing – original draft, Visualization, Validation, Software, Methodology, Investigation, Formal analysis, Data curation, Conceptualization. **M Angeles Clavero-Sanchez:** Investigation, Formal analysis. **Miguel Sánchez:** Investigation, Formal analysis. **Tiziana Missana:** Writing – review & editing, Visualization, Validation, Supervision, Software, Resources, Project administration, Methodology, Funding acquisition, Formal analysis, Data curation, Conceptualization.

Declaration of competing interest

The authors declare that they have no known competing financial interests or personal relationships that could have appeared to influence

the work reported in this paper.

Data availability

Data will be made available on request.

Acknowledgments

This project has received funding from the European Union's Horizon 2020 research and innovation program under grant agreement No 847593 and R+D Spanish national plan ARNO (PID2019-106398GB-I00).

Appendix A. Supplementary data

Supplementary data to this article can be found online at https://doi.org/10.1016/j.chemosphere.2024.143143.

References

Almendros-Ginestà, O., Missana, T., García-Gutiérrez, M., Alonso, U., 2023. Analysis of radionuclide retention by the cement hydrate phase portlandite: a novel modelling approach. Prog. Nucl. Energy 159, 104636. https://doi.org/10.1016/j.pnucene.2023.104636.

Atkins, M., Glasser, F.P., 1992. Application of portland cement-based materials to radioactive waste immobilization. Waste Management, Cementitious Materials in Radioactive Waste Management 12, 105–131. https://doi.org/10.1016/0956-053X(92)90044-J.

Atkinson, A., Everitt, N.M., Guppy, R.M., 1989. Time Dependence of pH in a Cementitious Repository. Materials Research Society, United States.

Belhadi, R., Govin, A., Grosseau, P., 2021. Influence of polycarboxylate superplasticizer, citric acid and their combination on the hydration and workability of calcium sulfoaluminate cement. Cement Concr. Res. 147, 106513 https://doi.org/10.1016/j.cemconres.2021.106513.

Bonin, L., Cote, G., Moisy, P., 2008. Speciation of An(IV) (Pu, Np, U and Th) in citrate media. Radiochimica Acta - RADIOCHIM ACTA 96, 145–152. https://doi.org/10.1524/ract.2008.1476.

Borkel, C., 2016. Understanding the mobility of caesium, nickel and selenium released from waste disposal : chemical retention mechanisms of degraded cement (Ph.D. Thesis). TDX (Tesis Doctorals en Xarxa). Universitat Politècnica de Catalunya.

Burešová, M., Kittnerová, J., Drtinová, B., 2023. Comparative study of Eu and U sorption on cementitious materials in the presence of organic substances. J. Radioanal. Nucl. Chem. 332, 1499–1504. https://doi.org/10.1007/s10967-022-08705-3.

Byrd, N., Lloyd, J.R., Small, J.S., Taylor, F., Bagshaw, H., Boothman, C., Morris, K., 2021. Microbial degradation of citric acid in low level radioactive waste disposal: impact on biomineralization reactions. Front. Microbiol. 12.

Carboneau, M.L., Adams, J.P., 1995. National Low-Level Waste Management Program Radionuclide Report Series, vol. 10. https://doi.org/10.2172/31669. Nickel-63 (No. DOE/LLW–126, 31669).

Courland, R., Smith, D., 2011. Concrete Planet: the Strange and Fascinating Story of the World's Most Common Man-Made Material. Amherst, N.Y.

Duarte, B., Delgado, M., Caçador, I., 2007. The role of citric acid in cadmium and nickel uptake and translocation, in Halimione portulacoides. Chemosphere 69, 836–840. https://doi.org/10.1016/j.chemosphere.2007.05.007.

Duque-Redondo, E., Yamada, K., Manzano, H., 2021. Cs retention and diffusion in C-S-H at different Ca/Si ratio. Cement Concr. Res. 140, 106294 https://doi.org/10.1016/j.cemconres.2020.106294.

Engel, M., Lezama Pacheco, J.S., Noël, V., Boye, K., Fendorf, S., 2021. Organic compounds alter the preference and rates of heavy metal adsorption on ferrihydrite. Sci. Total Environ. 750, 141485 https://doi.org/10.1016/j.scitotenv.2020.141485.

Galmarini, S., Bowen, P., 2016. Atomistic simulation of the adsorption of calcium and hydroxyl ions onto portlandite surfaces — towards crystal growth mechanisms. Cement Concr. Res. 81, 16–23. https://doi.org/10.1016/j.cemconres.2015.11.008.

Gavrilescu, M., Pavel, L.V., Cretescu, I., 2009. Characterization and remediation of soils contaminated with uranium. J. Hazard Mater. 163, 475–510. https://doi.org/10.1016/j.jhazmat.2008.07.103.

Giffaut, E., Grivé, M., Blanc, Ph, Vieillard, Ph, Colàs, E., Gailhanou, H., Gaboreau, S., Marty, N., Madé, B., Duro, L., 2014. Andra thermodynamic database for performance assessment: ThermoChimie. Applied Geochemistry, Geochemistry for Risk Assessment: Hazardous waste in the Geosphere 49, 225–236. https://doi.org/10.1016/j.apgeochem.2014.05.007.

Gonzalez-Siso, M.R., Duro, L., Bruno, J., Gaona, X., Altmaier, M., 2018. Thermodynamic model of Ni(II) solubility, hydrolysis and complex formation with ISA. Radiochim. Acta 106, 31–45.

Grambow, B., López-García, M., Olmeda, J., Grivé, M., Marty, N.C.M., Grangeon, S., Claret, F., Lange, S., Deissmann, G., Klinkenberg, M., Bosbach, D., Bucur, C., Florea, I., Dobrin, R., Isaacs, M., Read, D., Kittnerová, J., Drtinová, B., Vopálka, D., Cevirim-Papaioannou, N., Ait-Mouheb, N., Gaona, X., Altmaier, M., Nedyalkova, L., Lothenbach, B., Tits, J., Landesman, C., Rasamimanana, S., Ribet, S., 2020. Retention and diffusion of radioactive and toxic species on cementitious systems: main outcome of the CEBAMA project. Appl. Geochem. 112, 104480 https://doi.org/10.1016/j.apgeochem.2019.104480.

Guidone, R.E., Gaona, X., Winnefeld, F., Altmaier, M., Geckeis, H., Lothenbach, B., 2024. Citrate sorption on cement hydrates. Cement Concr. Res. 178, 107404 https://doi.org/10.1016/j.cemconres.2023.107404.

Hummel, W., Anderegg, G., Rao, L., Puigdomènech, I., Tochiyama, O., 2005. CHEMICAL THERMODYNAMICS of COMPOUNDS and COMPLEXES of U, Np, Pu, Am, Tc, Se, Ni and Zr with SELECTED ORGANIC LIGANDS 1130.

Iaea, I.A.E., 2001. Methods for the Minimization of Radioactive Waste from Decontamination and Decommissioning of Nuclear Facilities (Text), Methods for the Minimization of Radioactive Waste from Decontamination and Decommissioning of Nuclear Facilities. International Atomic Energy Agency.

Kar, A.S., Kumar, S., Tomar, B.S., 2012. U(VI) sorption by silica: effect of complexing anions. Colloids Surf. A Physicochem. Eng. Asp. 395, 240–247. https://doi.org/10.1016/j.colsurfa.2011.12.038.

Kastiukas, G., Zhou, X., Castro-Gomes, J., Huang, S., Saafi, M., 2015. Effects of lactic and citric acid on early-age engineering properties of Portland/calcium aluminate blended cements. Construct. Build. Mater. 101, 389–395. https://doi.org/10.1016/j.conbuildmat.2015.10.054.

Lee, C.A., van Veelen, A., Morris, K., Mosselmans, J.F.W., Wogelius, R.A., Burton, N.A., 2021. Uranium (VI) adsorbate structures on portlandite [Ca(OH)2] type surfaces determined by computational modelling and X-ray absorption spectroscopy. Minerals 11, 1241. https://doi.org/10.3390/min11111241.

Lenhart, J., Cabanis, S.E., McCarthy, P., Honeymann, B.D., 2000. Uranium (VI) complexation with citric, humic and fulvic acids. Radiochim. Acta 58, 5455–5463.

Loon, L.R.V., Glaus, M.A., 1998. Experimental and Theoretical Studies on Alkaline Degradation of Cellulose and its Impact Onthe Sorption of Radionuclides. Paul Scherrer Institut.

Ochs, M., Dolder, F., Tachi, Y., 2022. Decrease of radionuclide sorption in hydrated cement systems by organic ligands: comparative evaluation using experimental data and thermodynamic calculations for ISA/EDTA-actinide-cement systems. Appl. Geochem. 136, 105161 https://doi.org/10.1016/j.apgeochem.2021.105161.

Pasilis, S.P., Pemberton, J.E., 2008. Spectroscopic investigation of uranyl(VI) and citrate coadsorption to Al2O3. Geochem. Cosmochim. Acta 72, 277–287. https://doi.org/10.1016/j.gca.2007.09.036.

Seewald, J.S., Seyfried, W.E., 1991. Experimental determination of portlandite solubility in H2O and acetate solutions at 100–350 °C and 500 bars: constraints on calcium hydroxide and calcium acetate complex stability. Geochem. Cosmochim. Acta 55, 659–669. https://doi.org/10.1016/0016-7037(91)90331-X.

Taylor, H.F.W., 1997. Cement Chemistry. Thomas Telford.

Turgut, C., Katie Pepe, M., Cutright, T.J., 2004. The effect of EDTA and citric acid on phytoremediation of Cd, Cr, and Ni from soil using Helianthus annuus. Environ. Pollut. 131, 147–154. https://doi.org/10.1016/j.envpol.2004.01.017.

Van der Lee, J., de Windt, L., 1999. CHESS Tutorial and Cookbook (Technical Report No. LHM/RD/99/05). Ecole des Mines de Paris.

Verma, P.K., Pathak, P., Mohapatra, M., Yadav, A.K., Jha, S., Bhattacharyya, D., Mohapatra, P.K., 2015. Spectroscopic investigations on sorption of uranium onto suspended bentonite: effects of pH, ionic strength and complexing anions. Radiochim. Acta 103, 293–303. https://doi.org/10.1515/ract-2014-2309.

Zhang, G., Li, G., Li, Y., 2016. Effects of superplasticizers and retarders on the fluidity and strength of sulphoaluminate cement. Construct. Build. Mater. 126, 44–54. https://doi.org/10.1016/j.conbuildmat.2016.09.019.

Zou, D., Zhang, Z., Wang, D., 2020. Influence of citric acid and sodium gluconate on hydration of calcium sulfoaluminate cement at various temperatures. Construct. Build. Mater. 263, 120247 https://doi.org/10.1016/j.conbuildmat.2020.120247.